

A comprehensive model of a VLSI spiral inductor derived from the first principles

V.I. Kol'dyaev, S. Decoutere, R. Kuhn, and L. Deferm

IMEC, ASP division
Kapeldreef 75, B-3001 Leuven, Belgium.

Abstract

A wide-band 6-element lumped circuit is used to model spiral inductors. A decomposition of a spiral inductor into a set of bars is proposed to simulate the main spiral inductor parameters in a high-frequency range from 0.1 to 20 GHz. A method to simulate the main high-frequency parameters of a metal bar is proposed based on the use of 3D simulator "Raphael"(TMA). High-frequency 4 element distributed models with frequency dependent parameters are used in interpreting s-parameter measurements and simulating the input impedance. A model of the frequency dependent resistance of a metal bar due to the eddy currents in the substrate is developed. The excellent agreement between the simulation and experimental results indicates that the model is adequate for all the parameters.

1. Introduction

A simple formula to calculate the inductance of a spiral inductor (SI) is proposed in [1] but it does not permit to analyse the impact of a metal return path on the inductance if it is present, Fig.1, and to estimate the SI substrate capacitance for a specified SI layout. In [2-3], approximations are proposed for the calculation of the oxide C_0 and substrate C_S capacitances and the substrate resistance R_S . In this study the fundamental approach [4], to simulate the essentially three dimensional parameters C_0 , C_S , and R_S (see Fig.2-3), based on a solution of the 3D Laplace equation with proper boundary conditions is followed and its applicability is proven. Also the inductance is simulated based on a 3D-approximation from [4] using the TMA program "Raphael" [5] as a solver for a few stated boundary value problems. The impact of the boundary conditions is also studied.

2. Simulation approach

It is easy to show that the main parameters of the comprehensive high-frequency equivalent circuit shown in Fig.2(a), are frequency independent in the frequency range of 0.1 GHz to 20 GHz, except the total metal resistance R_m . The parasitic capacitance C_p and the total inductance L_T are of weak functions of f to be neglected in the first order approach. R_m is simulated in accordance to [6]. To simulate the inductance value the SI layout was decomposed into 20 bars as depicted in Fig.1: b0 to b19. The 2 matrices of the self- and mutual inductances for 2 sets of bars are simulated. The first set includes $b_i \{i=0,1,2,4,6,14-19\}$ and the second one has $b_j \{j=1,3,5,7, 9,11,13,17\}$. The contribution of the via's into L_T is neglected. Then these 2 matrices are properly combined to calculate the total inductance L_T . A SI design having a high-conductive return path is simulated taking the return path into account by decomposing it into extra bars (r1-r6) to be included in these 2 sets. In Fig.'s 4 and 5 a 2D presentation of the 3D-boundary value problems is depicted for the capacitances

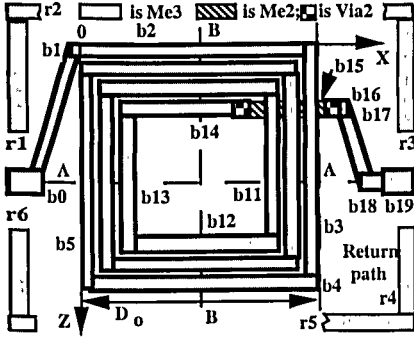


Figure 1: Layout of a square SI with the return path used in the simulation and measurements.

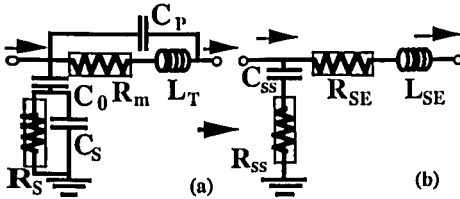


Figure 2: SI lumped physical equivalent circuit used in the simulation (a) and an equivalent circuit with frequency dependent elements used in s-parameter measurements (b).

the distances to the boundary conditions like d_t and d_a is studied to be correlated with a real environment of a SI in a circuit. The capacitances are studied in terms of 3 components: C_B , C_{PP} , C_A as depicted in Fig.4. After the main parameters were simulated the parasitic capacitance was extracted from the experimental resonance frequency of the input impedance. In order to extract the metal resistance versus frequency in the wide frequency range the Q-factor and the input impedance (Z_{in}) dependencies vs. f are proposed to be used because they are very sensitive to the metal resistance.

3. Simulation and experimental results

A set of SI's was experimentally studied. The SI design parameters are as follows: metal layer thickness $d_b=1 \mu\text{m}$ (Al), the substrate thickness $d_s=630 \mu\text{m}$, the substrate conductivity $0.05 \text{ 1}/\Omega\text{cm}$, the oxide thickness $d_{ox}=3.1 \mu\text{m}$, the metal width $W_b=17 \mu\text{m}$, the SI total length $D_t=2035 \mu\text{m}$. In Fig.6-9 the simulated and measured frequency behaviour of the main SI parameters are shown. The excellent agreement between the simulation and experimental results indicates that the developed physical and mathematical models for all the parameters are very accurate. C_p was determined from the resonance frequency in Fig.9 to be 29 fF .

In a frequency range below 1 GHz , the Q-factor is determined by the resistance of the SI metal line due to the carrier scattering process in metal R_{msc} , and the substrate losses due to the Maxwell-Wagner relaxation. In the range of $f > 1 \text{ GHz}$ the Q-factor is determined by a metal resistance which is described in [7] to be frequency dependent due to the skin-effect in

(C_0 and C_s) and the substrate resistance (R_s) simulation. To simulate R_s using the Laplace equation an artificial structure is created like an ideal contact to the substrate having the same layout as the SI layout. This is an approximation being applicable when $d_{ox} \ll d_s$ that is always fulfilled in real VLSI technologies. For the square SI layout a quarter of the total layout subdivided by quasi-symmetric lines "A" and "B" was used to reduce the simulation time. Moreover, for the R_s simulation the bars in the set were merged because of $d_{ox} \geq d_{sp}$, where d_{sp} is the spacing between the SI turns. The impact of

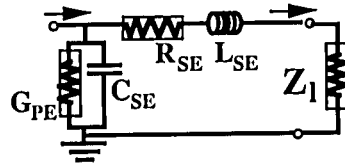


Figure 3: SI distributed equivalent circuit for Z_{in} . The distributed circuit parameters per unit length are frequency dependent and related to the parameters in Fig.2(a).

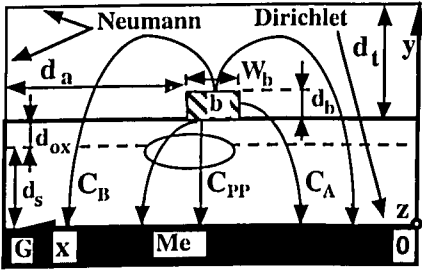


Figure 4: 2D-cross-section of a bar structure for C_0 (when d_s is put to be zero) and C_S simulation of the bar.

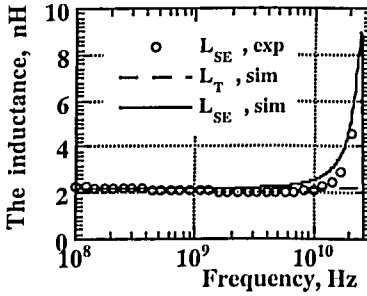


Figure 6: The simulated curve ("sim") and measured one ("exp") for the SI metal line inductance vs. frequency.

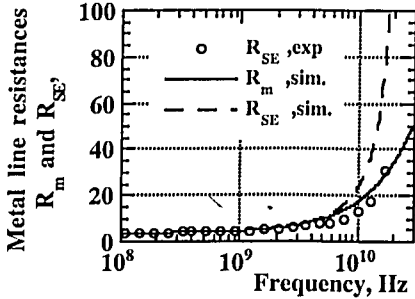


Figure 8: Simulated curves ("sim") and measured curve ("exp") for the SI metal line resistance vs. frequency.

the metal. According to [7] the frequency dependence follows a phenomenological law $R_m = R_{misc} + R(f)$, where $R(f) = R_0 f^b$, R_0 is constant and $b=1/2$ when the skin-effect is the dominant physical mechanism. However, experimentally b varied between 0.7 and 1.8 in [7] in contradiction to the skin-effect theory. Since in [7] the metal layer used was a $4 \mu\text{m}$ Au layer the impact of the skin-effect on the effective metal resistivity is difficult to distinguish from the

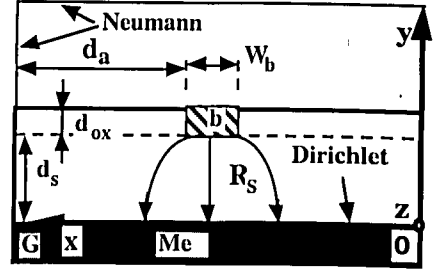


Figure 5: 2D-cross-section of the same bar structure as in Fig.4 for R_S simulation of the bar.

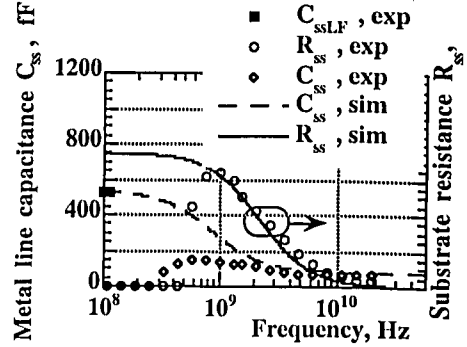


Figure 7: The simulated curves ("sim") and measured ones ("exp") for the SI metal line capacitance and the substrate resistance vs. frequency.

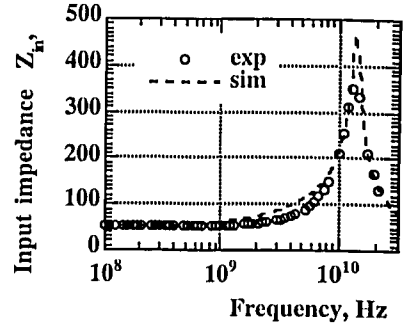


Figure 9: The simulated curve ("sim") and measured one ("exp") for the SI input impedance vs. frequency.

impact of the eddy current. In this study a thin metal layer ($d_b=1 \mu\text{m}$, Al) typical for VLSI interconnects was used, and it was found that $b=1.146$, see Fig.'s 10 and 11. This behaviour can be attributed to the eddy currents in the semiconductor substrate and it agrees with the theoretical estimation for b to be equal to 2 for a 1D-approximation [6] (see curve R_{mq} in Fig.11). A quasi-3D model for $R(f)=R_{mec}$ can be derived as follows: $R_{mec} = 2\pi\eta L_T \Psi(f)$, where $\Psi(f) = (2f/3f_{ss})$ and $f_{ss} = 1/(\pi\mu_0\sigma_s d_s^2)$ is the critical frequency for the 1D skin-effect in the substrate to take place. Since the value b is found to be 1.146 one has to interpret $\Psi(f)$ as follows: $\Psi(f) = [2f/3f_{ss}(f)] = h\sigma_s \cdot f^c$, where $c=0.146$ and the specific substrate thickness is hidden in $h=1.44 \text{ cm}/(\text{GHz})^c$. The frequency function $f_{ss}(f)$ is due to the 3D nature of the eddy currents because of $W_b \ll d_s$. It is worthwhile to note that the R_{mec} is proportional to the substrate conductivity. Since the typical thicknesses of VLSI substrates and dielectric layers are very close to d_s and d_{ox} used in this study, the extracted magnitude of h is expected to cover a wide range of practical spiral inductors and interconnects.

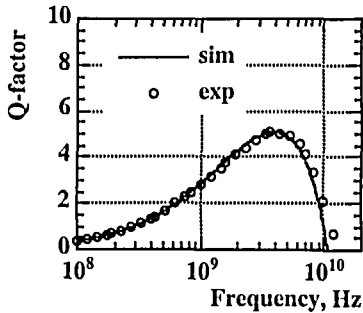


Figure 10: The simulated and measured Q-factor vs. frequency.

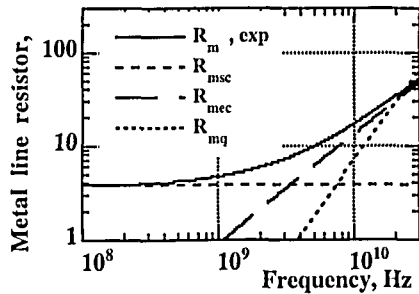


Figure 11: The metal resistance components vs. frequency.

4. Conclusions

The high accuracy model of spiral inductors is developed and its accuracy is proven by comparison with the original comprehensive experimental study. The developed approach is also applicable for a comprehensive interconnect simulation.

References

- [1] J.Crols, P.Kinget, J.Cranineckx et.al., "An analytical model of planar inductors on lowly doped silicon substrates," Symp.VLSI Circ.Dig.Tech.Pap., pp.28-31, 1996.
- [2] J.R. Long, M.A. Copeland, "The modeling, characterisation and design of monolithic inductors for silicon RFIC's," IEEE Jour. Solid State Circ., vol.32, no.3, pp.357-369, 1997.
- [3] C.P. Yue, C. Ryu, J. Lau, et.al., "A physical model for planar spiral inductors on silicon," IEDM'96, pp.155-158, 1996.
- [4] A.E.Ruchli, "Survey of computer-aided electrical analysis of integrated circuit interconnections," IBM J. Res.Develop., vol.23, no.6, pp.626-639, 1979.
- [5] "RAPHAEL", Interconnect analysis program, Reference Manual, ver.4, TMA, 1996.
- [6] H.Hasegawa, M. Furukawa, H. Yanai, "Properties of microstrip line on Si-SiO₂ system," IEEE Trans., vol.MTT-19, no.11, pp.869-881, 1972.
- [7] K.B. Ashby, I.A. Koullias, W.C. Finley, "High Q inductors for wireless applications in a silicon bipolar process," IEEE Jour. Sol.-St. Circuits, vol.31, no.1, pp.4-8, 1996.